Hyperon-rich matter in neutron stars

Jürgen Schaffner[1] and Igor N. Mishustin[1,2]
[1]*The Niels Bohr Institute, Blegdamsvej 17, DK-2100 Copenhagen, Denmark*
[2]*The Kurchatov Institute Russian Research Center, Moscow 123182, Russia*
(Received 19 June 1995)

We study the equation of state of hyperon-rich matter in neutron stars using an extended relativistic mean-field model. We take special care of the recently proposed nonlinear behavior of the vector field providing a much better agreement with Dirac-Brückner calculations. The hyperon-hyperon interaction is also implemented by introducing additional meson exchanges. With these new terms we avoid the instability found at high densities while keeping the excellent description for finite nuclear systems. We also demonstrate within the mean-field approach that the presence of hyperons inside neutron stars on one hand and the hyperon-hyperon interactions on the other hand make the onset of kaon condensation less favorable.

PACS number(s): 26.60.+c, 13.75.Ev, 21.65.+f, 95.30.Cq

I. INTRODUCTION

Nuclear matter at high densities and temperatures exhibits a new degree of freedom: strangeness, in neutron star matter hyperons and possibly kaons appear at a moderate density of about 2–3 times normal nuclear matter density $\rho_0 = 0.15$ fm^{-3}. These new species influence the properties of the equation of state of matter and the global properties of neutron stars. The relativistic mean-field (RMF) model has been used first by Glendenning for describing the equation of state of matter with hyperons [1]. There exist mainly two classes of parameter sets in the literature: the one fitted to nuclear matter properties and the other fitted to the properties of nuclei. The latter parameter sets suffer from several shortcomings: First, the parametrizations adjusted to reproduce the properties of nuclei fail at high densities due to an instability of the scalar self-interaction (for a general discussion see the work by Bodmer and Price [2], a possible solution to this problem has been suggested by Reinhard [3]). Second, compared to nonrelativistic or Dirac-Brückner calculations the equation of state is much stiffer, and the effective mass is much smaller ($m^*/m \approx 0.5$–0.6) at normal nuclear density which is unavoidable if the correct spin-orbit splitting is to be obtained [2]. A possible way out is to introduce a quartic self-interaction term for the vector field [4]. Such a model gives a good description of the properties of nuclei [5] and is in a reasonable agreement with Dirac-Brückner calculations [4,6]. In addition the instability found in the standard approach disappears. The equation of state for neutron stars (without hyperons) is considerably softened [4,5]. Third, the hyperon-hyperon interaction becomes important for hyperon-rich matter present in the dense interior of neutron stars (note that nearly equal abundances of hyperons and nucleons are predicted [1]). The standard RMF approach is not suited to reproduce the strongly attractive hyperon-hyperon interaction seen in double Λ hypernuclei. An improved Lagrangian incorporating an additional pair of (hidden) strange meson fields remedies the situation [7,8]. These additional interaction terms have never been applied for the equation of state of neutron star matter before.

When describing the properties of dense matter it is also necessary to study the possibility of pseudoscalar meson condensation. In particular, much attention has been paid in recent years to the kaon condensation in neutron stars [9]. Most recent calculations based on chiral perturbation theory [10,11] show that kaon condensation may set in at densities of 3–$4\rho_0$. Nevertheless, these calculations do not take into account the presence of hyperons which, as pointed out in [12], may already occupy a large fraction of matter when the kaons possibly start to condense. On the other side, the calculations including hyperons have not taken into account the possible kaon condensed phase. Only recently, some work has been started to incorporate the hyperon and kaon degrees of freedom at the same time [13,14]. In [13] the chiral Lagrangian by Kaplan and Nelson [9] is used for the baryons and kaons. The hyperons have not been included explicitly as constituents of the ground state, they are only considered through particle-hole excitations induced by the p-wave kaon-hyperon interaction. In this approach kaon condensation is predicted around $3\rho_0$. The other work [14] uses the standard relativistic mean-field (RMF) approach for the baryon sector and the kaon-baryon interactions from the Kaplan-Nelson Lagrangian. It is shown that the critical density for kaon condensation is shifted to higher densities when hyperons are included ($\rho_c > 4\rho_0$). It has been observed that due to the kaon condensate the nucleon effective mass acquires negative values at high densities. The authors conclude that the RMF model breaks down at these densities and that one has to go beyond the mean-field level. Thus, two approaches using the same kaon-baryon interactions come to different conclusions. In view of the present interest we also include the kaons in our RMF model by using kaon-baryon interactions motivated by meson exchange models. We demonstrate that the additional (hidden) strange meson fields mentioned above make kaon condensation less favorable even at very high densities.

The paper is organized as follows: In Sec. II we introduce the extended RMF model which includes hyperons in a controllable way by fitting the parameters to hypernuclear data. In addition the hyperon-hyperon interaction is introduced

through (hidden) strange meson exchanges. Then in Sec. III we apply the model for studying the equation of state of neutron star matter for representative parameter sets which cover more or less all presently available fits to the properties of nuclei and bulk matter. In Sec. IV we discuss the possibility of kaon condensation in neutron star matter. Section V is reserved for conclusions and outlook.

II. THE EXTENDED RMF MODEL

The relativistic mean-field (RMF) model is widely used now for describing finite nuclei as well as hot and dense nuclear matter (for recent reviews considering the case of nucleons see [15,16]). The RMF model for the full octet of baryons was first considered by Glendenning [1]. We start from the standard Lagrangian

$$\mathscr{L}=\sum_{\mathrm{B}}\bar{\Psi}_B(i\gamma^\mu\partial_\mu-m_B)\Psi_B+\frac{1}{2}\partial^\mu\sigma\partial_\mu\sigma-U(\sigma)-\frac{1}{4}G^{\mu\nu}G_{\mu\nu}+\frac{1}{2}m_\omega^2V^\mu V_\mu-\frac{1}{4}\vec{B}^{\mu\nu}\vec{B}_{\mu\nu}+\frac{1}{2}m_\rho^2\vec{R}^\mu\vec{R}_\mu-\sum_{\mathrm{B}}g_{\sigma B}\bar{\Psi}_B\Psi_B\sigma$$
$$-\sum_{\mathrm{B}}g_{\omega B}\bar{\Psi}_B\gamma^\mu\Psi_BV_\mu-\sum_{\mathrm{B}}g_{\rho B}\bar{\Psi}_B\gamma^\mu\vec{\tau}_B\Psi_B\vec{R}_\mu, \tag{1}$$

where the sum runs over all baryons of the baryon octet (p,n, $\Lambda,\Sigma^+,\Sigma^0,\Sigma^-,\Xi^0,\Xi^-$). The term $U(\sigma)$ stands for the scalar self-interaction

$$U(\sigma)=\frac{1}{2}m_\sigma^2\sigma^2+\frac{b}{3}\sigma^3+\frac{c}{4}\sigma^4 \tag{2}$$

introduced by Boguta and Bodmer [17] to get a correct compressibility of normal nuclear matter. The parameters of this Lagrangian have been fitted to the properties of finite nuclei [18,19]. It turned out that the best fits are obtained for the parameter sets with $c<0$. In this case the functional form (2) of the scalar field potential leads to an instability at high densities. Its traces are already seen in the nucleus ^{12}C [3]. Hence, another stabilized functional form has been given by Reinhard [3] which eliminates the instability while keeping the good description of nuclei, especially the spin-orbit splitting. Alternatively, Bodmer proposed an additional self-interaction term for the vector field [4] of the form

$$\mathscr{L}_{V^4}=\frac{1}{4}d(V_\mu V^\mu)^2. \tag{3}$$

This modification leads to a nice agreement with Dirac-Brückner calculations at high densities [6]. The reason is that the vector field is then proportional to $\rho^{1/3}$ in contrast to the linear dependence in the standard model. The fits to the properties of nuclei are quite successful and the instability due to the scalar self-interaction vanishes [5]. Below we adopt this modification.

The implementation of hyperons is straightforward. The corresponding new coupling constants have been fitted to hypernuclear properties [20]. It turns out that the two coupling constants of the Λ ($g_{\sigma\Lambda}$ and $g_{\omega\Lambda}$) are strongly correlated because they are fixed by the depth of the Λ potential

$$U_\Lambda^{(N)}=g_{\sigma\Lambda}\sigma^{\mathrm{eq}}+g_{\omega\Lambda}V_0^{\mathrm{eq}} \tag{4}$$

in saturated nuclear matter [21,22]. Here $U_i^{(j)}$ denotes the potential depth of a baryon species i in matter of baryon species j. Hence one can use for example SU(6) symmetry for the vector coupling constants

$$\frac{1}{3}g_{\omega N}=\frac{1}{2}g_{\omega\Lambda}=\frac{1}{2}g_{\omega\Sigma}=g_{\omega\Xi},$$
$$g_{\rho N}=\frac{1}{2}g_{\rho\Sigma}=g_{\rho\Xi}, \tag{5}$$
$$g_{\rho\Lambda}=0$$

and fix the scalar coupling constants to the potential depth of the corresponding hyperon in normal nuclear matter. Following [7,8] we choose

$$U_\Lambda^{(N)}=U_\Sigma^{(N)}=-30\ \mathrm{MeV},\quad U_\Xi^{(N)}=-28\ \mathrm{MeV} \tag{6}$$

in accordance with the available hypernuclear data. The potential depth of the Σ is assumed to be the same as for the Λ. Based on analyses of Σ^- atomic data it was found that the real part of the optical potential is $-(25$–$30)$ MeV [23]. A recent analysis [24] indicates that the potential changes sign in the nuclear interior, i.e., being repulsive instead of attractive. We will discuss implications of this repulsive potential depth for our results but we will stick mainly to the choice given in Eq. (6) which constitutes our model 1.

Nevertheless, this model is not able to reproduce the observed strongly attractive $\Lambda\Lambda$ interaction irrespectively of the chosen vector coupling constant. An extensive discussion about the measured strong $\Lambda\Lambda$ interaction can be found in [25]. The situation can be remedied by introducing two additional meson fields, the scalar meson $f_0(975)$ (denoted as σ^* in the following) and the vector meson $\phi(1020)$ with the masses given in parenthesis [7,8]. The corresponding Lagrangian reads

$$\mathscr{L}^{YY}=\frac{1}{2}(\partial_\nu\sigma^*\partial^\nu\sigma^*-m_{\sigma^*}^2\sigma^{*2})-\frac{1}{4}S_{\mu\nu}S^{\mu\nu}$$
$$+\frac{1}{2}m_\phi^2\phi_\mu\phi^\mu-\sum_B g_{\sigma^*B}\bar{\Psi}_B\Psi_B\sigma^*$$
$$-\sum_B g_{\phi B}\bar{\Psi}_B\gamma_\mu\Psi_B\phi^\mu. \tag{7}$$

The vector coupling constants to the ϕ field are given by SU(6) symmetry (see [8] for details)

$$2g_{\phi\Lambda}=2g_{\phi\Sigma}=g_{\phi\Xi}=-\frac{2\sqrt{2}}{3}g_{\omega N},\quad g_{\phi N}=0. \tag{8}$$

The scalar coupling constants to the σ^* field are fixed by the condition

$$U_{\Xi}^{(\Xi)}\approx U_{\Lambda}^{(\Xi)}\approx 2U_{\Xi}^{(\Lambda)}\approx 2U_{\Lambda}^{(\Lambda)}\approx -40\quad \text{MeV} \tag{9}$$

which is motivated by the one-boson exchange model D of the Nijmegen group and the measured strong $\Lambda\Lambda$ interaction [8]. Note that the nucleons are not coupled to these new fields. In the following we denote the extended model with hyperon-hyperon interactions as model 2.

We conclude this section with a brief comment concerning the limitations of the RMF model. This is clearly an effective model which successfully describes nuclear phenomenology in the vicinity of the ground state. On the other hand, this model does not respect chiral symmetry and the quark structure of baryons and mesons. Also negative energy states of baryons and quantum fluctuations of meson fields are disregarded. These deficiencies may affect significantly the extrapolations to high temperatures, densities, or strangeness contents.

III. NEUTRON STAR MATTER WITH HYPERONS

A. Equilibrium conditions

The equation of state for neutron star matter is derived by standard methods (see, e.g., [1] for the RMF approach without the hidden strange meson fields). The equations of motion for the meson fields in uniform matter at rest are given by

$$m_{\sigma}^2\sigma+\frac{\partial}{\partial\sigma}U(\sigma)=\sum_{\mathrm{B}} g_{\sigma B}\rho_S^{(B)}, \tag{10}$$

$$m_{\sigma^*}^2\sigma^*=\sum_{\mathrm{B}} g_{\sigma^* B}\rho_S^{(B)},$$

$$m_{\omega}^2V_0+dV_0^3=\sum_{\mathrm{B}} g_{\omega B}\rho_V^{(B)},$$

$$m_{\rho}^2R_{3,0}=\sum_{\mathrm{B}} g_{\rho B}\tau_3^B\rho_V^{(B)},$$

$$m_{\phi}^2\phi_0=\sum_{\mathrm{B}} g_{\phi B}\rho_V^{(B)},$$

where ρ_S and ρ_V denote the scalar and vector densities, respectively. The equations can be solved for a given total baryon density ρ_B and charge density ρ_c including the contributions from the free electrons and muons

$$\rho_B=\sum_{\mathrm{B}} \rho_V^{(B)},$$

$$\rho_c=\sum_{\mathrm{B}} q_B\rho_V^{(B)}+\sum_{l=e,\mu} q_l\rho_l=0, \tag{11}$$

where q_i stands for the electric charge of a species i. In β equilibrium the chemical potentials of the particles are related to each other by

$$\mu_i=b_i\cdot\mu_B+q_i\cdot\mu_e, \tag{12}$$

where b_i is the baryon number of a species i. This means that all reactions which conserve charge and baryon number are allowed, as, e.g.,

$$n+n\rightarrow\Lambda+n,\quad \Lambda+\Lambda\rightarrow\Xi^-+p,\ldots. \tag{13}$$

Since we consider neutron stars on a long time scale, the strangeness quantum number is not constrained and the net strangeness is determined by the condition of β equilibrium. The above equations fix the fields and the equilibrium composition of neutron star matter. The energy density and pressure can be derived from the grand canonical potential or the energy-momentum tensor in a standard way (see, e.g., [1]) and the generalization to the additional fields is straightforward:

$$\epsilon=\frac{1}{2}m_{\sigma}^2\sigma^2+\frac{b}{3}\sigma^3+\frac{c}{4}\sigma^4+\frac{1}{2}m_{\sigma^*}^2\sigma^{*2}+\frac{1}{2}m_{\omega}^2V_0^2+\frac{3}{4}dV_0^4+\frac{1}{2}m_{\rho}^2R_{3,0}^2+\frac{1}{2}m_{\phi}^2\phi_0^2+\sum_{i=B,l}\frac{\nu_i}{(2\pi^3)}\int_0^{k_F^i}d^3k\sqrt{k^2+m_i^{*2}}, \tag{14}$$

$$P=-\frac{1}{2}m_{\sigma}^2\sigma^2-\frac{b}{3}\sigma^3-\frac{c}{4}\sigma^4-\frac{1}{2}m_{\sigma^*}^2\sigma^{*2}+\frac{1}{2}m_{\omega}^2V_0^2+\frac{1}{4}dV_0^4+\frac{1}{2}m_{\rho}^2R_{3,0}^2+\frac{1}{2}m_{\phi}^2\phi_0^2+\sum_{i=B,l}\frac{\nu_i}{(2\pi^3)}\int_0^{k_F^i}d^3k\frac{k^2}{\sqrt{k^2+m_i^{*2}}}, \tag{15}$$

TABLE I. The coupling constants of the parameter sets used in the calculations. The vector coupling constants for the hyperons are taken from SU(6) relations. The nucleons do not couple to the σ^* and ϕ mesons ($g_{\sigma^* N}=g_{\phi N}=0$). The Λ does not couple to the isovector fields ($g_{\rho\Lambda}=0$). The coupling constants for the Σ's are the same as for the Λ except for the isovector coupling constant which is $g_{\rho\Sigma}=2g_{\rho N}$. The parameters for the scalar and vector self-interaction terms are not given, they can be found in the corresponding references. For the set GL85 we choose $m_\omega=780$ MeV, $m_\rho=763$ MeV, and a σ-meson mass of 500 MeV.

Set	NL-Z	NL-SH	PL-Z	PL-40	TM1	TM2	GL85
Ref.	[18]	[19]	[3]	[3]	[5]	[5]	[1]
$g_{\sigma N}$	10.0553	10.4440	10.4262	10.0514	10.0289	11.4694	7.9954
$g_{\omega N}$	12.9086	12.9450	13.3415	12.8861	12.6139	14.6377	9.1462
$g_{\rho N}$	4.8494	4.3830	4.5592	4.8101	4.6322	4.6783	4.8139
$g_{\sigma\Lambda}$	6.23	6.47	6.41	6.20	6.21	7.15	4.96
$g_{\omega\Lambda}$	8.61	8.63	8.89	8.59	8.41	9.76	6.10
$g_{\sigma^*\Lambda}$	6.77	6.85	6.93	6.78	6.67	7.65	5.11
$g_{\phi\Lambda}$	-6.09	-6.10	-6.29	-6.07	-5.95	-6.90	-4.31
$g_{\sigma\Xi}$	3.45	3.59	3.52	3.43	3.49	3.94	2.97
$g_{\omega\Xi}$	4.30	4.31	4.45	4.30	4.20	4.88	3.05
$g_{\rho\Xi}$	4.85	4.38	4.56	4.81	4.63	4.68	4.81
$g_{\sigma^*\Xi}$	12.59	12.66	12.95	12.57	12.35	14.18	9.38
$g_{\phi\Xi}$	-12.17	-12.20	-12.58	-12.15	-11.89	-13.80	-8.62

where

$$m_B^*=m_B+g_{\sigma B}\sigma+g_{\sigma^* B}\sigma^* \tag{16}$$

is the effective mass of the baryon B (for leptons the vacuum mass is taken).

B. Composition of matter

In the following we study the composition and the equation of state of neutron star matter for the various parameter sets obtained from fits to finite nuclei. The corresponding coupling constants are listed in Table I.

In principle one can also use parameter sets fitted to the bulk properties of nuclear matter and to the asymmetry energy. These sets usually have a higher effective mass than the former ones. When using these parametrizations no negative effective masses occur in neutron star matter [1]. Nevertheless, all parameter sets used in the following describe more or less the properties of nuclear matter and give a reasonable strong spin-orbit term. This in turn implies a small effective mass as discussed in [2]. For comparison we consider also the parametrization used by Glendenning (GL85) [1] where the parameters are fixed to the bulk properties of nuclear matter (see Table I). Table II shows the nuclear matter properties corresponding to the different parameter sets used.

First we take the sets NL-Z (which is set NL-1 with a more consistent center-of-mass correction [18]), NL-SH [19] for the Boguta model, and the sets PL-40 and PL-Z [3] with the stabilized scalar functional. The first parameter set shows a well-known instability at high densities [3] which appears in neutron star matter around $\rho\approx 0.5$ fm^{-3}. At this point the effective mass of the nucleon gets negative due to the presence of the hyperons. For higher density no solution can be found. Negative effective nucleon masses appear also for set NL-SH at a density of $\rho\approx 0.8$ fm^{-3} for model 1 and at 1.0 fm^{-3} for model 2. The same holds for the case with the stabilized functional forms, sets PL-Z and PL-40 [3], in models 1 and 2 around a similar density region. Note that this happens even without the presence of a kaon condensate as found in [14]. One might wonder about the fact that the early occurrence of negative masses found here has not been seen in [14]. The explanation is simple: The standard parameter sets from fits to finite nuclei always favor a stiff equation of state to get a correct spin-orbit splitting which inhibits this

TABLE II. The nuclear matter properties of the parameter sets used. The saturation density and the energy are denoted by ρ_0 and E/A, the incompressibility by K, the effective mass by m_N^*/m_N and the symmetry energy by $a_{\rm sym}$.

Set	NL-Z	NL-SH	PL-Z	PL-40	TM1	TM2	GL85
Ref.	[18]	[19]	[3]	[3]	[5]	[5]	[1]
ρ_0 (fm^{-3})	0.151	0.146	0.153	0.152	0.145	0.132	0.145
E/A (MeV)	-16.2	-16.3	-15.9	-16.2	-16.3	-16.2	-15.95
K (MeV)	172	355	294	166	281	344	285
m_N^*/m_N	0.583	0.597	0.55	0.58	0.634	0.571	0.77
$a_{\rm sym}$ (MeV)	41.8	36.1	40.5	41.7	36.9	35.8	36.8

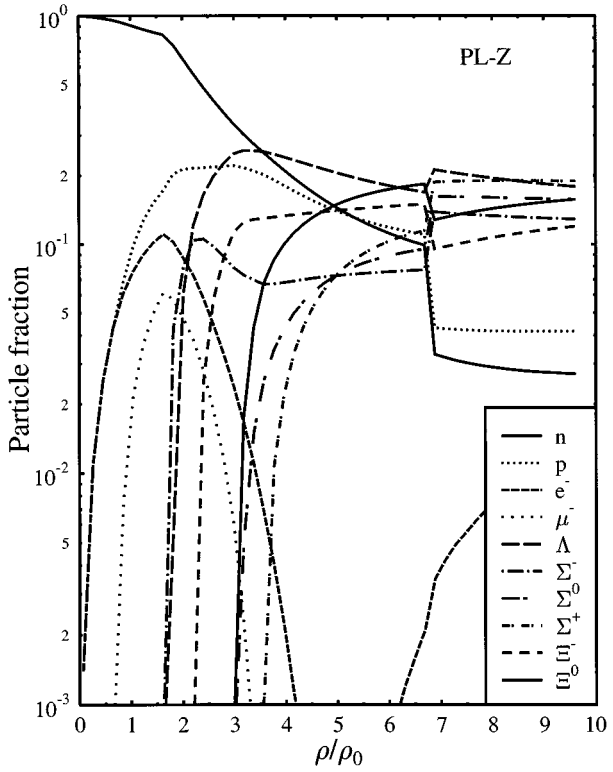

FIG. 1. The composition of neutron star matter with hyperons in model 2 using parameter set PL-Z. The jump in the curves is due to the negative effective mass of the nucleon.

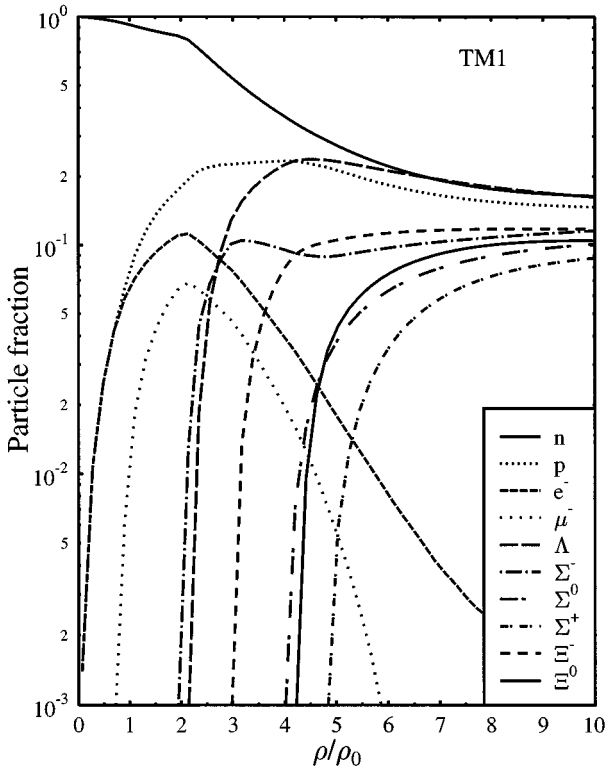

FIG. 2. The composition of neutron star matter with hyperons in model 2 using parameter set TM1 with vector self-interaction terms. The matter approaches isospin-hypercharge-saturation at high densities.

instability as the fields are growing fast with the density. Fits to nuclear matter only can lead to a rather soft equation of state which avoids the instability due to a moderate rise of the fields. Nevertheless, the latter parametrizations are not able to describe the strong spin-orbit splitting seen in finite nuclei (for a detailed discussion see [2,18]) and therefore cannot be considered as realistic. In the following we extended our calculation to densities beyond the instability by taking always the absolute value $|m_N^*|$ of the effective mass. It is clear that a much more refined procedure is necessary to treat the problem of negative effective masses, i.e., going beyond the standard mean-field approximation. But this is beyond the scope of the present work.

The behavior for lower densities is quite similar in all these models. Figure 1 shows as an example the composition of neutron star matter for the set PL-Z and model 2. The proton fraction rises rapidly and reaches maximum values over 20% around $2–3\rho_0$. At this density, the hyperons, first Λ's and Σ^-'s then Ξ^-'s, appear abundantly and the lepton fraction is considerably reduced. When the other hyperons are present at densities of $3–4\rho_0$ the number of Λ's even exceeds the number of neutrons, so that the dense interior resembles more a hyperon star than a neutron star. Also the population of leptons gets negligibly low, as the electrochemical potential drops instead of growing. These general features have been found earlier by Glendenning [1]. Nevertheless, in our calculation all the hyperons are settled in earlier compared to the findings in [1]. We have also checked for the occurrence of Ω^- which do not contribute in any of our calculations.

The situation at higher densities differs for the various parameter sets mainly due to the instability mentioned above. Taking the absolute value of the nucleon effective mass one still cannot find a solution for the sets NL-Z and NL-SH above the critical density for model 1. For the sets PL-Z and PL-40 we found a solution where the neutron star matter becomes pure hyperon matter dominated by Λ's and no nucleons appear above the critical density. Also the electrochemical potential changes sign and positrons and antimuons appear instead of electrons and muons. When turning on the hyperon-hyperon interactions (model 2) the hyperons feel effectively an additional repulsion at these high densities. Hence, nucleons are now present but still considerably less abundant than hyperons. Now a solution for set NL-SH can be also found. Nevertheless, these results should be taken with some precaution as we do not treat the problem of negative effective masses consistently.

Now we turn our discussion to the case of models with vector self-interactions. Two sets, named TM1 and TM2, exist so far in the literature [5] (see also Table I). It has already been found that the behavior of the nuclear equation of state follows more closely the trends of relativistic Brückner-Hartree-Fock calculations and that the maximum mass of a neutron star is reduced [4,5]. Figure 2 shows the composition of neutron star matter for the set TM1 with hyperons and with hyperon-hyperon interactions (model 2). Up to the maximum density considered here, $10\rho_0$, all effective masses remain positive and no instability occurs. The behavior at moderate densities is quite close to that of the previous

parametrizations: The proton fraction has a plateau at $2-4$ ρ_0 and exceeds 20% which allows for the direct URCA process and a rapid cooling of the neutron star [26]. Hyperons, first Λ's and Σ^-'s, appear at $2\rho_0$, then Ξ^-'s are populated already at $3\rho_0$. The number of electrons and muons has a maximum at this density here. The muons vanish when all the hyperons have been settled at $\rho \approx 0.85$ fm^{-3} while the electrons remain on the level of 2% . The fractions of all baryons show a tendency towards saturation, they asymptotically reach similar values of 8–15 % which correspond approximately to spin-isospin and hypercharge-saturated matter. In the ideal case of vanishing effective masses all baryon fractions would be proportional to the spin-degeneracy factors.

Switching off the hyperon-hyperon interactions, i.e., going from model 2 to model 1, we see again that negative effective masses appear at $\rho = 1.3$ fm^{-3} for set TM1 and at $\rho = 0.95$ fm^{-3} for set TM2 due to the missing additional repulsive force for the hyperons. Nevertheless, the main population pattern is not changed considerably below $\rho = 0.6$ fm^{-3} when going from model 2 to model 1, but the number of hyperons, especially Λ's, are reduced at higher densities. Also the leptons vanish for set TM1, but for the set TM2 positrons appear again, as the electrochemical potential changes sign above the occurrence of the instability. These results demonstrate the importance of the additional exchanges by σ^* and ϕ mesons. An additional repulsion is needed here at higher densities to stabilize neutron star matter.

For comparison we preformed the calculations also for the parameter set GL85 from Glendenning [1]. Figure 3 shows the composition of neutron star matter for model 2. The behavior looks quite similar compared to the other parameter sets except for the Σ's which are suppressed here. Also no negative effective masses occur. The effective masses of the baryons are higher, e.g., at $10\rho_0$ the effective mass of the nucleon is still around 300 MeV whereas it is close to zero for the other parameter sets (see Fig. 4). Hence the effective mass term still plays a dominant role favoring Λ's and Ξ's. Note that the Ξ's see only a half of the repulsive vector potential from the ω meson compared to the Σ's. We find a quite similar behavior also for model 1.

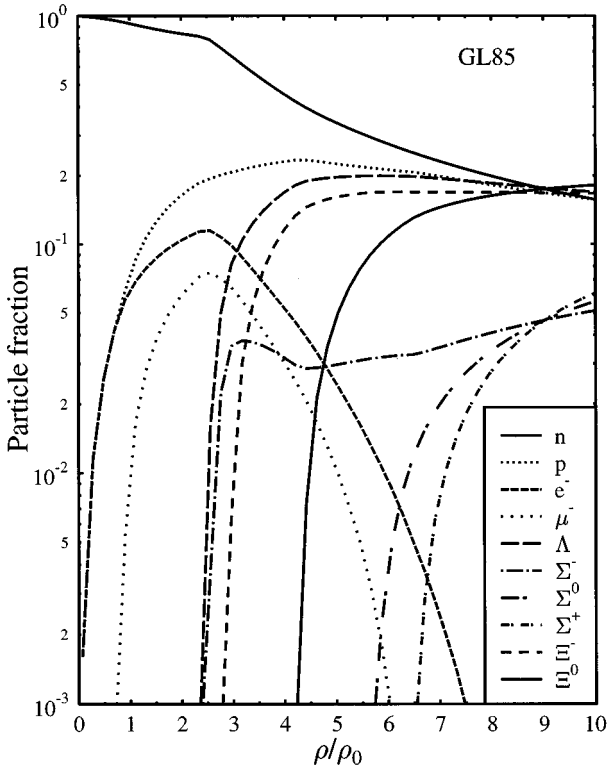

FIG. 3. The composition of neutron star matter with hyperons in model 2 using the parameter set GL85. The abundances of all species become equal at high densities except for the Σ's which are suppressed.

C. Baryon effective masses and field potentials

The effective masses defined in (16) are plotted in Fig. 4 for the various baryons for set TM1 and model 2. The effective mass of the nucleons reaches rapidly very small values and then saturates at higher densities never reaching negative values. For hyperons the behavior is quite similar but less pronounced as their coupling constants to the σ field are smaller than for nucleons. Nevertheless, the combined effect of the σ and σ^* fields results in a rather constant gap between the effective masses over the whole density range shown. Note that the nucleons do not couple to the (hidden) strange scalar field σ^*. The overall small masses of the baryons at very high densities indicate that the neutron star matter approaches an isospin-hypercharge-saturated state matter with close abundances, as seen in Fig. 2.

The pure scalar and vector field strengths are shown in Fig. 5. To get the potential for a given baryon species they have to be multiplied by the corresponding coupling constants listed in Table I. In addition, we have also plotted the electrochemical potential. It reaches a maximum value of about 200 MeV around $\rho \approx 2-3\rho_0$ and then gets considerably lower at high densities instead of growing steadily. This behavior is due to the onset of negatively charged hyperons (Σ^- and Ξ^-) as has been first found by Glendenning [1]. The vector potential exhibits initially a linear rise which then slows down due to the vector self-interaction and the onset of hyperons at $\rho \approx 0.3$ fm^{-3}. At the same density the (hidden) strange fields are developed and reach quite high values for very dense matter. The ϕ field shows a rather linear behavior with density while the scalar fields tend to saturation at high densities. The isovector-vector field induced by the ρ exchange is quite small over the whole density range and never exceeds -15 MeV. The other fields are one order of magnitude higher and have opposite signs. This also indicates a large cancellation between scalar and vector terms. The fields get so strong, that, for example, a 10% change of one coupling constant can alter the potential up to 100 MeV. Therefore, it is very important to fine tune the scalar coupling constants according to the potential depth [see Eqs. (6) and (9)]. This has to be kept in mind for the forthcoming discussion of the properties of kaons in dense neutron star matter.

D. Equation of state

The pressure versus the energy density is shown in Fig. 6

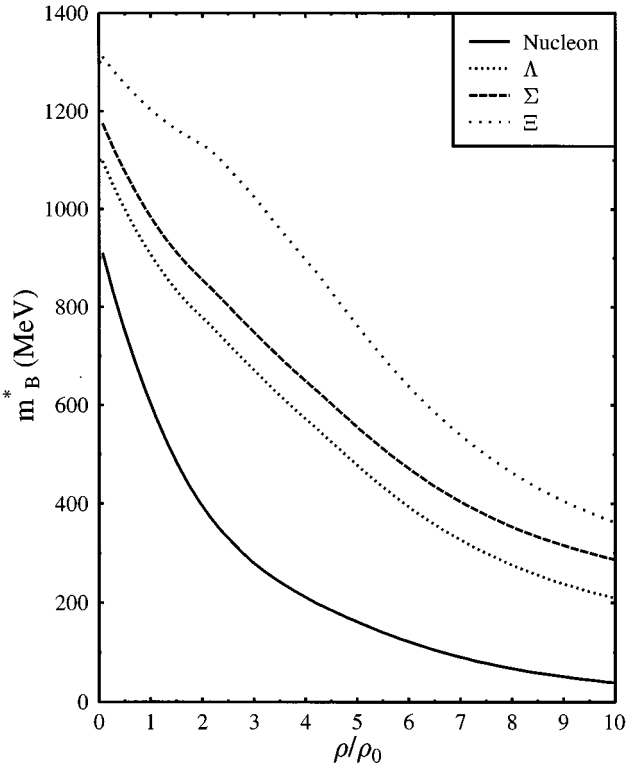

FIG. 4. The effective masses of the baryons vs the density for model 2 using set TM1. All effective masses remain positive for the density range considered.

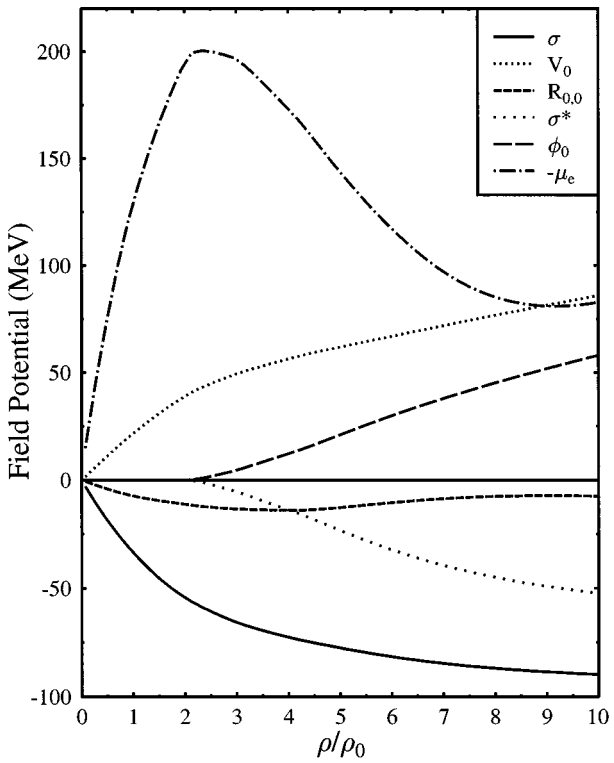

FIG. 5. The mean meson fields and the electrochemical potential vs the density for model 2 using set TM1. Scalar and vector fields have opposite signs indicating large cancellation effects at high densities.

for all parameter sets using model 2. For $\epsilon<800$ MeV fm^{-3} there exist mainly two bunches of curves. The parameter sets without vector self-interaction are located in the upper branch. The sets TM1 and TM2 with vector self-interaction are softer, i.e., they have a lower pressure for a given energy density and are therefore constituting the lower branch of curves. For higher energy densities, set TM2 is stiffer than set TM1. Also the parameter set GL85 fitted to bulk properties of nuclear matter is rather soft and is located in the lower branch of curves. For the upper branch one recognizes kinks in the curves which are due to the instability discussed above (i.e., negative effective masses). For model 1 (not shown), one sees a very pronounced jump in the curves due to the occurrence of this instability. The equation of state gets then considerably softened reaching very low pressures. But for model 2 the jump is much less pronounced and even vanishes for the sets with vector self-interaction. Another difference between model 1 and model 2 is the slight softening of the equation of state for intermediate densities which is due to the attractive hyperon-hyperon interaction mediated by the σ^*-meson exchange. For very high densities model 2 gets stiffer than model 1, because the contribution from the repulsive ϕ field overwhelms now the attraction from the σ^* field which is saturating at very high densities. In addition the stiffest possible equation of state $\epsilon=p$ is also drawn. The causality condition $\partial p/\partial\epsilon\leqslant 1$ is fulfilled by all sets, so that the sound velocity remains lower than the speed of light. The microscopic stability condition $\partial p/\partial\epsilon\geqslant 0$ is also satisfied except for the instability regions associated with negative effective masses.

We have also calculated neutron star matter using the coupling constants for the Σ's derived from a most recent analysis of Σ^- atomic data [24] and checked for changes. We used set TM1 with the coupling constants $g_{\omega\Sigma}=g_{\omega N}$ and $g_{\rho\Sigma}=2/3g_{\rho N}$ instead of the ones given in Eq. (5) and took a repulsive potential depth of $U_\Sigma^{(N)}=+30$ MeV at normal nuclear density. Mainly due to the higher coupling constant to the ω meson we find that the Σ's do not appear in our calculation at all. This demonstrates the sensitivity of the composition of neutron star matter to a small change of the coupling constants. Nevertheless, the proton fraction still exceeds 20% allowing for the direct URCA process. All remaining baryons approach equal abundances for high densities. The changes in the effective masses, field potentials, electrochemical potential and the equation of state are very small (less than 10%) compared to our previous results. The electrochemical potential is a little bit higher and the equation of state gets a little bit stiffer at high densities. Also the results for the in-medium energy of the kaon shown in the next section do not change significantly when applying these coupling constants.

E. Effects of the δ meson

Finally, we want to study possible extensions of the RMF approach by including other mesons. It is well known that pseudoscalar and pseudovector mesons do not contribute in the mean-field approximation. The same holds for all the kaon resonances as they couple off-diagonally. Tensor meson fields also vanishes in infinite matter. Hence, the only re-

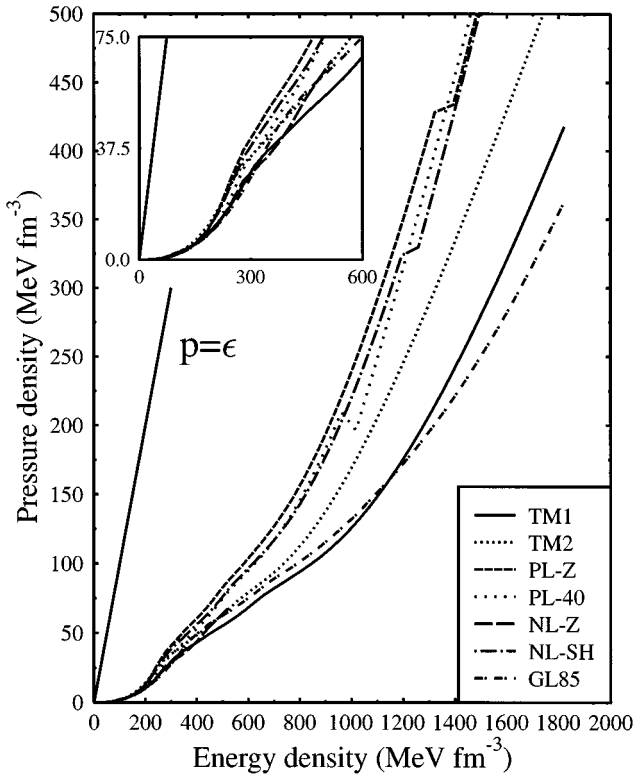

FIG. 6. The equation of state of neutron star matter with hyperons in model 2 for different parameter sets. The low density regime is zoomed up. The causal limit $p=\epsilon$ is also shown.

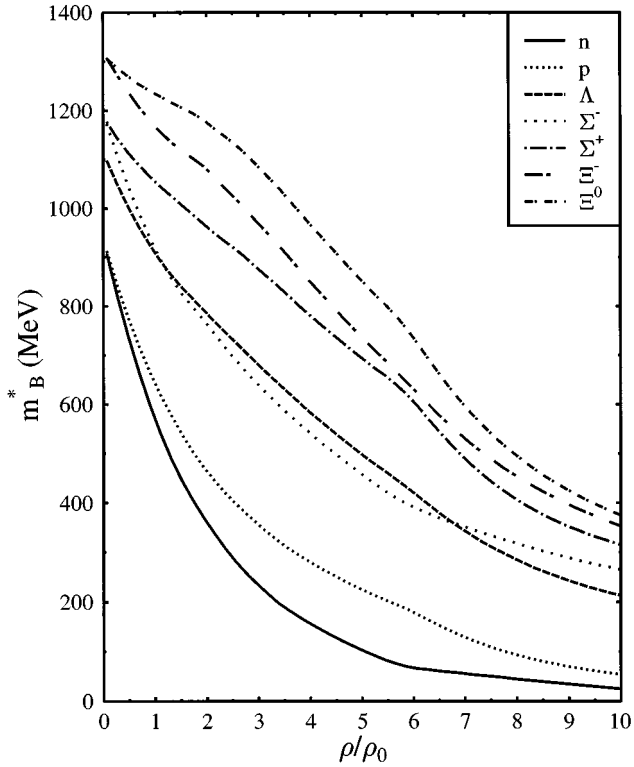

FIG. 7. The effective masses of the baryons versus the density for model 2 using set TM1 with δ mesons. All baryons have different (nondegenerate) effective masses due to the δ-meson contribution.

maining meson which can be added to the present Lagrangian is the scalar isovector meson $a_0(980)$ (the δ meson). To our knowledge this meson has been not considered so far for the equation of state of neutron stars. Fits to the properties of nuclei seem to indicate that its contribution are negligible for the discussion about binding energy, radius and surface thickness of stable nuclei [18]. Nevertheless, it might be important for very asymmetric systems. For the discussion in the next section it is instructive to study the influence of this meson on the properties of neutron star matter. We implemented the δ meson in the standard way with the coupling constant $g_{\delta N}=5.95$ taken from the Bonn model [27]. The other coupling constants are scaled according to the isospin of the corresponding baryon ($2g_{\delta N}=g_{\delta\Sigma}=2g_{\delta\Xi}$, $g_{\delta\Lambda}=0$). As seen in Fig. 5 the contribution from the vector isovector meson ρ is quite negligible compared to the other fields. Therefore, we expect only minor changes when introducing the scalar isovector meson δ. Indeed, the equation of state with the δ meson gets only a little bit stiffer for lower density regions. For higher densities the equation of state approaches the one for symmetric matter and the contribution of the δ meson simply vanishes in this case. The baryon composition shows some small changes for densities lower than $\rho<3\rho_0$. As the δ field is repulsive for the protons, but attractive for the Σ^-'s, the former ones are a little bit suppressed while the latter ones appear slightly earlier. These effects reduce the number of electrons and the maximum chemical potential is now about 150 MeV instead of 200 MeV. The other meson fields do not change when the δ field is introduced. The most pronounced effect, despite the lower electrochemical potential, is the change in the effective masses of the baryons which are plotted in Fig. 7. In contrast to Fig. 4 every baryon has now a different effective mass. The biggest effect is seen for the Σ^- due to its large coupling constant to the δ field. The effective mass of the Σ^- can even be lower than that of the Λ. The neutron has a significantly lower effective mass compared to the proton. For high densities the relative difference can be as large as a factor of 2. The absolute difference can exceed 120 MeV. Nevertheless, the potential induced by the δ field never exceeds 70 MeV for the nucleons and is therefore negligible compared to the rather high potential terms coming from the isoscalar fields (see Fig. 5).

IV. KAON INTERACTION IN THE HYPERON-RICH MEDIUM

A. Preliminary remarks

The kaon-nucleon interaction has been studied recently within different approaches including the Bonn model [28], the Nambu-Jona-Lasinio model [29], and chiral perturbation theory [30]. Antikaons in dense nuclear matter are of special interest because they can form a condensate [9] leading to a considerable softening of the equation of state and a reduction of the maximum mass of neutron stars [10]. But this issue is still controversial. The chiral perturbation theory gives a rather robust prediction for the onset of antikaon condensation at $\rho_c\approx 3$–$4\rho_0$ [11]. However, a simple consid-

eration based on the RMF model leads to a strong nonlinear density dependence of the antikaon energy disfavoring antikaon condensation [12].

We highly appreciate many efforts for constructing a consistent approach to kaon condensation based on the chiral perturbation theory [11,30,31]. But in our opinion this approach has principal difficulties which may not be easy to overcome in the near future. The main problem is that simple chiral models have never been applied successfully for describing the saturation properties of nuclear matter. By this reason the parameters used for calculating the kaon energy (coupling constants, nucleon effective mass, etc.) may not be consistent with the properties of the background nuclear matter. Another and maybe related problem is that only linear terms in the baryon density are under control in the chiral Lagrangian. In particular, the scalar density ρ_s is identified with the baryon (vector) density ρ of the matter in the leading order expansion of the chiral Lagrangian. This approximation certainly fails at high densities (for instance at $\rho \approx 3\rho_0$ the difference can be about 80% [3]). Already using the scalar density, as it is dictated by Lorentz invariance, shifts the kaon condensation threshold to densities above $5\rho_0$ [12,32]. In [12] it was also shown that many-body forces associated with the self-interaction of the meson fields disfavor kaon condensation even more. By these reasons we use a more phenomenological approach in the present paper based on the one-boson exchange model.

As it is well known, there exists an important difference between K^+N and K^-N interaction. Compared to K^+N the K^-N interaction is more complicated due to the existence of the $\Lambda(1405)$ resonance just below threshold. This makes the interpretation of the available K^-N scattering and K^- atomic data less transparent. Recently an improved fit of K^- atomic data was carried out assuming a nonlinear density dependence of the effective t matrix [33]. It has been shown that the real part of the antikaon optical potential can be as attractive as

$$U_{\rm opt}^{\bar{K}} \approx -200 \pm 20 \ \ {\rm MeV} \tag{17}$$

at normal nuclear matter density while being slightly repulsive at very low densities. This fit is in agreement with the low density theorem for K^-p scattering and is strongly affected by the $\Lambda(1405)$ resonance. Also another family of solutions has been found with a moderate potential around -50 MeV. Note that the standard linear extrapolation gives only values of about -85 MeV [33]. These latter two solutions do not fulfill the low density theorem, i.e., they are not getting repulsive at low densities. There exist some hints that the $\Lambda(1405)$ is a quasibound state in the t channel [34,28]. It is not surprising then that the K^-N scattering data can be explained by a simple vector meson exchange [34] where the effects of this resonance come out automatically. This resonance seems to be less important in dense matter when the kaon mass is shifted down below $m_{\Lambda(1405)} - m_N \approx 465$ MeV. In [35] a separable potential was applied for the K^-p interaction for finite density. Indeed, it was found that the mass of the $\Lambda(1405)$ is shifted upwards and exceeds the K^-p threshold already at densities of about $\rho \approx 0.4\rho_0$. In this case the use of mean-field potentials may be justified. Most recently, the $\Lambda(1405)$ has been also included in the chiral approach [31]. No effect has been found for the onset of kaon condensation [31], but one should note that the $\Lambda(1405)$ has been only implemented as a new elementary particle contrary to the conclusion drawn in [34,28]. In a recent paper Kaiser, Siegel, and Weise have applied a coupled channel analysis for chiral perturbation theory [36]. Within this formalism the $\Lambda(1405)$ is automatically generated and the low energy K^-p scattering data are successfully described.

In our previous work [12] we have conjectured an important role which hyperons should play in determining the threshold of kaon condensation. Here we present the calculations which confirm these qualitative estimates. Recently, the effects of the presence of hyperons have been studied also by Ellis, Knorren, and Prakash [14]. The authors use the RMF model with scalar self-interaction for the baryon sector and the chiral approach of Kaplan and Nelson [9] for the kaon-baryon interaction. It has been shown that the presence of hyperons, in particular the Σ^-, shifts the threshold for K^- condensation by several units of ρ_0. Note, however, that Ellis *et al.* do not take into account the off-shell terms which are necessary for a correct description of the KN-scattering lengths [11]. As we will show below, these additional terms will shift the onset of kaon condensation to even higher densities.

B. Kaon effective energy

In the following we adopt the meson-exchange picture for the KN interaction simply because we use it also for parametrizing the baryon interactions. By analogy to the Bonn model [28] the simplest kaon-meson Lagrangian can be written as

$$\begin{aligned}\mathscr{L}_K = {} & \partial_\mu \bar{K} \partial^\mu K - m_K^2 \bar{K} K - g_{\sigma K} m_K \bar{K} K \sigma \\ & - g_{\sigma^* K} m_K \bar{K} K \sigma^* - g_{\omega K} \bar{K} i \overleftrightarrow{\partial}_\mu K V^\mu - g_{\rho K} \bar{K} \vec{\tau}_K i \overleftrightarrow{\partial}_\mu K \vec{R}^\mu \\ & - g_{\phi K} \bar{K} i \overleftrightarrow{\partial}_\mu K \phi^\mu . \end{aligned} \tag{18}$$

However, it is easy to see that this coupling scheme does not fulfill the Ward identity in the medium requiring that the vector field should be coupled to a conserved current. Indeed, the conserved kaon current from the Lagrangian (18) reads

$$\begin{aligned} j_\mu^K &= i \left(\bar{K} \frac{\partial \mathscr{L}}{\partial^\mu \bar{K}} - \frac{\partial \mathscr{L}}{\partial^\mu K} K \right) \\ &= \bar{K} i \partial_\mu K - (i \partial_\mu \bar{K}) K - 2 \bar{K} K (g_{\omega K} V_\mu + g_{\rho K} \vec{\tau} \vec{R}_\mu + g_{\phi K} \phi_\mu), \end{aligned} \tag{19}$$

where the third term would not be present in free space. From the equation of motion for the vector field V^μ one has

$$\partial_\mu F^{\mu\nu} + m_\omega^2 V^\nu = \sum_{\rm B} g_{\omega B} \overline{\Psi}_B \gamma^\nu \Psi_B + g_{\omega K} (\bar{K} i \overleftrightarrow{\partial}_\nu K) \tag{20}$$

and after applying a partial derivative on both sides

$$m_\omega^2 \partial_\nu V^\nu = \sum_{\rm B} g_{\omega B} \partial_\nu (\overline{\Psi}_B \gamma^\nu \Psi_B) + g_{\omega K} \partial^\nu (\bar{K} i \overleftrightarrow{\partial}_\nu K) \tag{21}$$

(the vector self-interaction term is omitted here because it is purely phenomenological and the following arguments do not hold for it). The first term on the right-hand side vanishes due to the baryon number conservation which is fulfilled for every baryon species for strong interactions. The second term would also vanish in vacuum, but not in the medium. The situation changes when introducing the modified kaon-meson Lagrangian

$$\mathscr{L}'_K = D^*_\mu \bar{K} D^\mu K - m_K^2 \bar{K} K - g_{\sigma K} m_K \bar{K} K \sigma - g_{\sigma^* K} m_K \bar{K} K \sigma^* \tag{22}$$

with the covariant derivative

$$D_\mu = \partial_\mu + i g_{\omega K} V_\mu + i g_{\rho K} \vec{\tau} \vec{R}_\mu + i g_{\phi K} \phi_\mu . \tag{23}$$

One gets now additional terms of the form

$$\mathscr{L}'_K = \mathscr{L}_K + (g_{\omega K} V_\mu + g_{\rho K} \vec{\tau} \vec{R}_\mu + g_{\phi K} \phi_\mu)^2 \bar{K} K. \tag{24}$$

These terms modify the equations of motion for the vector fields in such a way that, e.g.,

$$m_\omega^2 \partial_\mu V^\mu = \sum_B g_{\omega B} \partial_\mu j_B^\mu + g_{\omega K} j_K^\mu = 0. \tag{25}$$

It should be emphasized that the additional terms are not forced by Eq. (25) (for a discussion about fixing the zero component of the vector field see [37]) but by the Ward identity. The equation of motion for kaons in uniform matter then reads

$$\{\partial_\mu \partial^\mu + m_K^2 + g_{\sigma K} \sigma m_K + g_{\sigma^* K} \sigma^* m_K + 2(g_{\omega K} V_0 + g_{\rho K} \tau_3 R_{3,0} + g_{\phi K} \phi_0) i \partial^\mu - (g_{\omega K} V_0 + g_{\rho K} \tau_3 R_{3,0} + g_{\phi K} \phi_0)^2\} K = 0, \tag{26}$$

where we have used Eq. (25). The coupling constants to the vector mesons are chosen from the SU(3) relations

$$2 g_{\omega K} = 2 g_{\rho K} = \sqrt{2} g_{\phi K} = g_{\pi\pi\rho} = 6.04. \tag{27}$$

Decomposing the kaon field into plane waves one obtains the following dispersion relation for kaons (upper sign) and antikaons (lower sign) in uniform matter composed of nucleons and hyperons

$$\omega_{K,\bar{K}} = \sqrt{m_K^2 + m_K (g_{\sigma K} \sigma + g_{\sigma^* K} \sigma^*) + k^2} \pm (g_{\omega K} V_0 + g_{\phi K} \phi_0 + g_{\rho K} \tau_3 R_{3,0}). \tag{28}$$

Note that due to the additional term (24) the vector potentials appear linearly in the kaon energy.

The coupling constant $g_{\sigma K}$ could be taken from the Bonn model [28] but here we adopt another prescription. We fix it to the value of the potential depth of kaons in the nuclear medium to reproduce the strongly attractive potential seen in kaonic atoms [33]. The optical potential in symmetric nuclear matter ($R_{3,0}=0$, $\sigma^*=0$, $\phi_0=0$, no hyperons, $k=0$) can be reconstructed from the equation of motion (26)

$$2 \mu_{KN} U_{\rm opt}^{\bar{K}} = g_{\sigma K} \sigma m_K - 2 g_{\omega K} \omega_{\bar{K}} V_0 - (g_{\omega K} V_0)^2, \tag{29}$$

where μ_{KN} is the reduced mass of the $K^- N$ system. By comparing with Eq. (28) one notices that in general the optical potential and the energy shift (relative to the free mass) of the (anti)kaon do not coincide. In addition, the right-hand side of Eq. (29) shows a nonlinear density dependence (see also [33]). At normal nuclear density the in-medium energy shift of the antikaon is about 20% less than the corresponding optical potential.

In the following we consider two possibilities: we adjust the scalar coupling constant to $U_{\rm opt}^{\bar{K}} = -120$ MeV, as an upper bound for the standard fit and the lower family of solutions found in [33], or to $U_{\rm opt}^{\bar{K}} = -200$ MeV for the second family of solutions. Note that the deep optical potential family is linked to the $\Lambda(1405)$ physics. Hence one should consider this deep potential as more appropriate. On the other hand, once the energy is lowered with increasing density, the $\Lambda(1405)$ becomes irrelevant and perhaps its contribution to the K^- optical potential should be ignored. This would suggest a weakening of the optical potential under increasing the density.

In our approach the low density theorem is not fulfilled for the $\bar{K}N$ case due to the presence of the $\Lambda(1405)$ resonance (in principle, one has to solve coupled channel equations to get the correct scattering length, which is beyond the scope of this paper). We argue here that the contribution of the $\Lambda(1405)$ can be neglected for the evaluation of K^- nuclear interaction at high densities, when the energy of the $K^- N$ system drops below 1405 MeV (see also [33,35]). This implicitly contains the assumption that the mass of the $\Lambda(1405)$ stays constant with growing density.

C. Onset of kaon condensation

The onset of s-wave kaon condensation is determined by the condition

$$-\mu_e = \mu_{K^-} \equiv \omega_{K^-}(k=0). \tag{30}$$

When calculating μ_{K^-} we have also taken into account the contribution from the (hidden) strange meson fields σ^* and ϕ_0 according to Eq. (28). The coupling constant to the σ^* field has been determined from $f_0(975)$ decay [38], $g_{\sigma^* N} = 2.65$. Note that this value is obtained despite the fact that the mass of the f_0 is lower than the $K\bar{K}$ threshold which is a source of uncertainty. While the σ^* field is attractive, the ϕ field is repulsive for antikaons. In a hyperon-rich medium the contribution of the ϕ field is always repulsive for hyperons and K^- while attractive for antihyperons and K^+. This can be traced back to the strangeness number which is $S=-1$ for hyperons and K^- but $S=+1$ for antihyperons and K^+. The isovector field is also repulsive for the K^- since neutrons (and also Σ^-) are more abundant than protons (and Σ^+). As seen in Fig. 6 the electrochemical potential goes through a maximum and then decreases at higher densities.

The relativistic effects, the reduced electrochemical potential, and the presence of the ϕ- and the ρ-meson fields make kaon condensation less favorable for hyperon-rich matter. Interestingly, that already Glendenning [1] has referred to this decrease of the electrochemical potential as a reason why kaons are not likely to condense.

In Fig. 8 we plot $\omega_{K^-} - \mu_{K^-}$ as a function of baryon density for model 2 and the various parameter sets considered

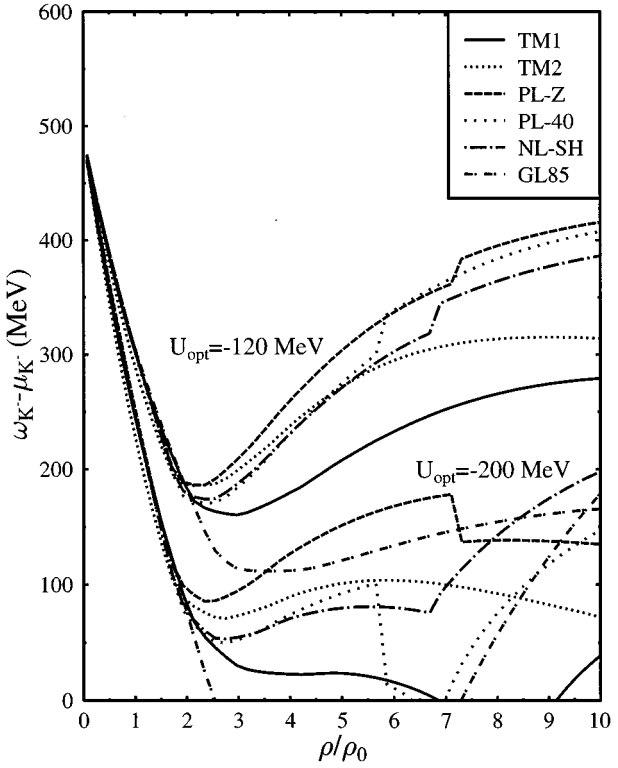

FIG. 8. The effective energy minus the chemical potential of the K^- vs the baryon density for model 2 using various parameter sets. The upper curves are calculated for a K^- optical potential at normal density of $U_{\rm opt}^{\bar{K}}=-120$ MeV, the lower ones for $U_{\rm opt}^{\bar{K}}=-200$ MeV.

above. The upper curves correspond to $U_{\rm opt}^{\bar{K}}=-120$ MeV whereas the lower curves to $U_{\rm opt}^{\bar{K}}=-200$ MeV. Below $2\rho_0$ one sees a rather steep and linear drop. After the appearance of hyperons, the slope of the curves changes dramatically and they even turn upward again. Antikaon condensation is only possible if a curve crosses zero. This does not happen at all for the upper family of curves and only occurs for set PL-40 (but in the unstable regime with negative effective masses), for sets TM1 and GL85 among the lower family. The almost linear decrease of the effective kaon energy in the latter case, among other reasons (see the discussion in [12]), may be explained by the rather huge scalar coupling constant of the kaon, $g_{\sigma K}=6.5$, which is close to the one for the nucleon. As the vector potential gives only about 50 MeV attraction, the scalar potential must be unrealistically deep, about -175 MeV, to get $U_{\rm opt}^{\bar{K}}=-200$ MeV [see Eq. (29)]. Note that the two sets TM1 and TM2, which do not get negative effective masses and might be the most reliable calculations, give different predictions concerning the possibility of kaon condensation. While the former one reaches zero at $\rho\approx 6\rho_0$, the latter one is at all densities at least 60 MeV above the critical value.

The only conclusion, which one can make after inspecting Fig. 8, is that theoretical predictions for the antikaon energy are rather uncertain above $2\rho_0$. A better determination of the K^- optical potential in nuclei is extremely important for reducing this uncertainty.

The kaon optical potential presented in the previous section is unsatisfactory in several respects. First, it does not fulfill the low density constraints on the scattering lengths. Second, for the case of $U_{\rm opt}^{\bar{K}}=-200$ MeV the optical potential of the K^+ meson turns out to be attractive while experiment tells us that it is repulsive. And third, the off-shell behavior of the KN-scattering amplitude is not correct. Hence, below we consider possible ways of eliminating these shortcomings.

D. Fitting scattering lengths

Alternatively to the procedure used in the previous sections, one can fix the parameters of the kaon Lagrangian to the $\bar{K}N$-scattering lengths. The $\bar{K}N$ case can be obtained by performing a G-parity transformation. For the Lagrangian (22) the isospin averaged scattering length in the tree approximation reads [39]

$$\bar{a}_0=\frac{1}{4}a_0^{I=0}+\frac{3}{4}a_0^{I=1}$$
$$=\frac{m_K}{4\pi(1+m_K/m_N)}\left(\frac{g_{\sigma K}g_{\sigma N}}{m_\sigma^2}-2\frac{g_{\omega K}g_{\omega N}}{m_\omega^2}\right)$$
$$=-0.255\text{fm}, \tag{31}$$

where the experimental value has been taken from [40]. It can be used to fix $g_{\sigma K}$ for known $g_{\omega K}$. Nevertheless, the Lagrangian (22) is not able to give the correct KN-scattering length in the two isospin channels separately. A way out might be in introducing in addition to the ρ meson, an extra coupling of the kaon to the scalar isovector meson $a_0(980)$ which we denote as δ. The KN-scattering lengths for a given isospin I on the tree level are then given by

$$a_0^{I=1}=\frac{m_K}{4\pi(1+m_K/m_N)}\left(\frac{g_{\sigma K}g_{\sigma N}}{m_\sigma^2}+\frac{g_{\delta K}g_{\delta N}}{m_\delta^2}\right.$$
$$\left.-2\frac{g_{\omega K}g_{\omega N}}{m_\omega^2}-2\frac{g_{\rho K}g_{\rho N}}{m_\rho^2}\right), \tag{32}$$

$$a_0^{I=0}=\frac{m_K}{4\pi(1+m_K/m_N)}\left(\frac{g_{\sigma K}g_{\sigma N}}{m_\sigma^2}-3\frac{g_{\delta K}g_{\delta N}}{m_\delta^2}\right.$$
$$\left.-2\frac{g_{\omega K}g_{\omega N}}{m_\omega^2}+6\frac{g_{\rho K}g_{\rho N}}{m_\rho^2}\right). \tag{33}$$

The necessity of the δ-meson exchange contribution can be seen if one first sets it to zero and take SU(6) symmetry for the vector coupling constants. Then the ω and ρ contributions cancel out ($g_{\omega K}g_{\omega N}=3g_{\rho K}g_{\rho N}$) and the $a_0^{I=0}$ scattering length contains only the term coming from the σ-meson exchange. This gives a large positive scattering length whereas the experimental value [40], $a_0^{I=0}=-0.09$ fm, is slightly negative. Taking $g_{\sigma N}=10$, $g_{\omega N}=13$ as standard values for the RMF model (see Table I) one gets $a_0^{I=0}\approx 0.4$ fm without the δ-meson contribution. Including the δ-meson term and using $g_{\delta N}=5.95$ from the Bonn model [27] one can fit both scattering lengths nicely for

TABLE III. The coupling constants for the interactions of kaons with different mesons. The coupling constants to the σ and δ meson are fixed by the s-wave KN-scattering lengths. The vector coupling constants are chosen from SU(3) relations. The coupling constant to the σ^* meson is taken from f_0 decay [38].

Set	NL-Z	NL-SH	PL-Z	PL-40	TM1	TM2	GL85
Ref.	[18]	[19]	[3]	[3]	[5]	[5]	[1]
$g_{\sigma K}$	1.85	2.05	2.20	2.27	1.93	2.27	1.27
$g_{\omega K}$	3.02	3.02	3.02	3.02	3.02	3.02	3.02
$g_{\rho K}$	3.02	3.02	3.02	3.02	3.02	3.02	3.02
$g_{\sigma^* K}$	2.65	2.65	2.65	2.65	2.65	2.65	2.65
$g_{\phi K}$	4.27	4.27	4.27	4.27	4.27	4.27	4.27
$g_{\delta K}$	6.37	5.59	5.89	6.31	5.87	5.94	6.31

$$g_{\sigma K}\approx 1.9-2.3, \quad g_{\delta K}\approx 5.6-6.4 \tag{34}$$

for the various parameter sets used. A complete list of the coupling constants of the kaon can be found in Table III. Note that the values are surprisingly close to the ones expected from the simple quark-model ($g_{\sigma K}=g_{\sigma N}/3\approx 3.3$, $g_{\delta K}=g_{\delta N}=5.95$). Set GL85 gives a smaller value for $g_{\sigma K}$ compared to the other parameter sets which is related to the smaller $g_{\omega N}$ value (see Table III). The effects of the δ meson on the properties of neutron star matter were discussed in the previous section and seemed to be quite insignificant. Hence, despite the rather large coupling constant to the δ meson its influence on the kaon effective energy in neutron star matter is expected to be rather small compared with the other isoscalar fields.

E. Off-shell effects

Effective chiral Lagrangians, which incorporate a correct off-shell behavior of the KN-scattering amplitude, have been proposed in [11,41]. These two approaches introduce different off-shell terms. But despite that, as shown in [42], the effective meson masses can be uniquely obtained. In our approach we do not need off-shell terms to get the correct KN-scattering lengths. Hence, the coupling constants for the off-shell terms cannot be fixed unambiguously. Here we simply adopt the view that the scalar term in the KN amplitude has to change sign when going from the on-shell point $\omega_K=m_K$ to the off-shell point $\omega_K=0$ as outlined in [41] and check the importance of the off-shell terms for the onset of kaon condensation. In the one-boson exchange picture this can be achieved by introducing the following terms:

$$\mathscr{L}_K''=D_\mu^*\bar{K}D^\mu K\left(\frac{f_{\sigma K}\sigma}{m_K}+\frac{f_{\sigma^* K}\sigma^*}{m_K}\right)+D_\mu^*\bar{K}\vec{\tau}D^\mu K\frac{f_{\delta K}\vec{\delta}}{m_K}. \tag{35}$$

The on-shell constraints, Eqs. (32) and (33), can still be fulfilled if one replaces $g_{\sigma K}$ by $g_{\sigma K}-f_{\sigma K}$ and $g_{\delta K}$ by $g_{\delta K}-f_{\delta K}$, respectively, and uses for $g_{\sigma K}-f_{\sigma K}$ and $g_{\delta K}-f_{\delta K}$ the values given in (34). The scalar part of the off-shell amplitude is now proportional to

$$\propto\left(1-\frac{f_{\sigma K}}{g_{\sigma K}}\frac{\omega_K^2}{m_K^2}\right)\frac{g_{\sigma K}g_{\sigma N}}{m_\sigma^2}m_K.$$

According to [41] it changes sign for $\omega=m_K/\sqrt{2}$, if one takes $f_{\sigma K}=2g_{\sigma K}$. Together with the condition $g_{\sigma K}-f_{\sigma K}\approx 2$ this gives $g_{\sigma K}\approx -2$ and $f_{\sigma K}\approx -4$. Note that in [11] the off-shell terms are smaller, $f_{\sigma K}/g_{\sigma K}=-m_K^2 D'/\Sigma_{KN}\approx 0.4$, so that both coupling constants are positive. With the new terms (35) the effective mass of the kaon in the hyperon-free medium is

$$m_K^{*2}=\frac{m_K^2+g_{\sigma K}\sigma m_K}{1+f_{\sigma K}\sigma/m_K} \tag{36}$$

(note that both the scalar fields and the coupling constants are negative here). It is reduced compared to the case $f_{\sigma K}\approx 0$ and $g_{\sigma K}\approx 2$ so that it makes kaon condensation even less favorable at higher densities.

We have found that the fit based on the adjustment to the $K\bar{N}$-scattering lengths leads to a $\bar{K}$-optical potential around $U_{\rm opt}^{\bar{K}}=-(130\text{–}150)$ MeV at normal nuclear density for the parameter sets used. This is between the two families of solutions found in [33]. Set GL85 gives a much shallower optical potential of $U_{\rm opt}^{\bar{K}}=-96$ MeV.

The general expression for the effective energy of the charged kaon (plus sign) and the antikaon (minus sign) in neutron star matter is given by

$$\omega_{K^+,K^-}=m_K\sqrt{\frac{m_K+g_{\sigma K}\sigma+g_{\sigma^* K}\sigma^*\pm g_{\delta K}\tau_3\delta_0}{m_K+2(g_{\sigma K}\sigma+g_{\sigma^* K}\sigma^*\pm g_{\delta K}\tau_3\delta_0)}}$$
$$\pm(g_{\omega K}V_0+g_{\phi K}\phi_0+g_{\rho K}\tau_3 R_{3,0}). \tag{37}$$

The density dependence of the K and $\bar{K}$ effective energies is displayed in Fig. 9 for the parameter sets TM1, TM2, and GL85 using model 2 with the δ meson. The two cases (with and without the off-shell terms) are shown. The energy of the kaon is first increasing in accordance with the low density theorem. The energy of the antikaon is decreasing steadily at low densities. With the appearance of hyperons the situation changes dramatically. The potential induced by the ϕ field cancels the contribution coming from the ω meson. Hence, at a certain density the energies of the kaons and antikaons become equal to the kaon (antikaon) effective mass, i.e., the curves for kaons and antikaons are crossing at a sufficiently high density. At higher densities the energy of the kaon gets even lower than that of the antikaon. The difference between the two parameter sets considered is not as important as the

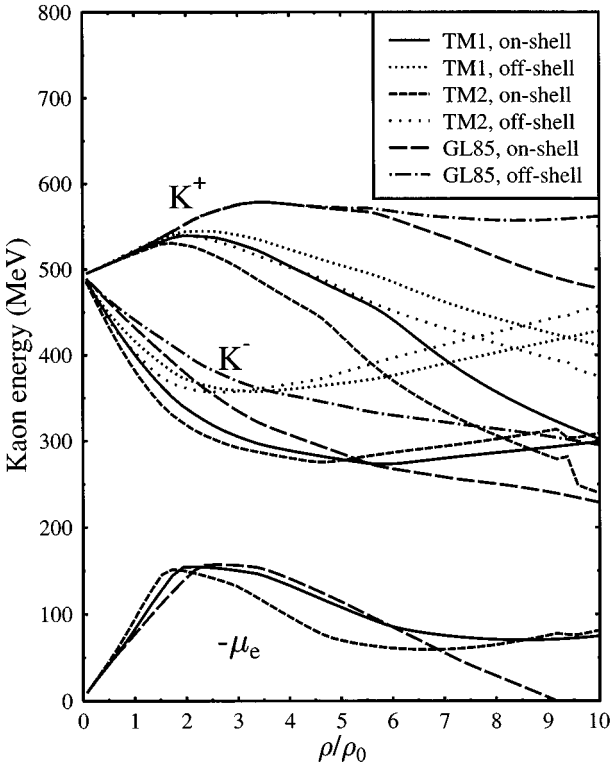

FIG. 9. The effective energy of the kaon and the antikaon for model 2 with δ mesons using sets TM1, TM2, and GL85. The calculations with and without off-shell terms are shown. The electrochemical potential is also plotted. Antikaon condensation does not occur over the whole density region considered.

inclusion of the off-shell terms. These terms shift noticeably the effective mass of the kaon to higher values. Accordingly the in-medium energy of both kaons and antikaons is shifted up by at most 100 MeV. The minimum energy of the antikaon reaches about 270 MeV for the on-shell and 350 MeV for the off-shell case. Since the chemical potential never reaches values above 160 MeV here (or 200 MeV without the δ meson), antikaon condensation does not occur either with or without off-shell terms. We have checked the possibility of antikaon condensation for all parameter sets for model 1 and model 2 and found that at least 100 MeV are missing for the onset of condensation also for set GL85. For the latter parameter set we see no crossing but a saturation of the effective antikaon energy around 230 MeV for the on-shell and 300 MeV for the off-shell case. The most uncertain term for the effective energy of the antikaon is the one coming from the σ^* exchange. If one arbitrarily doubles the coupling constant this would lead at maximum to an additional attraction of about 70–80 MeV and still no antikaon condensation is possible within our approach.

V. CONCLUSION AND OUTLOOK

We have studied the equation of state of neutron star matter within the relativistic mean-field model including hyperons. We have used representative sets of parameters fixed by the properties of nuclei and nuclear bulk matter. In addition we have included the rather strong hyperon-hyperon interaction induced by additional (hidden) strange meson fields. The coupling constants of the hyperons have been fixed by SU(6)-symmetry relations and hypernuclear properties. Parameter sets fitted to properties of nuclei with different forms of the scalar self-interaction yield negative values for the nucleon effective mass due to the abundant presence of hyperons at high densities. The vector self-interaction terms and the additional meson exchanges together eliminate this behavior. According to our calculations, the baryon effective masses become small in neutron star matter at very high densities ($\rho > 6\rho_0$) and the abundances of different species are determined by their spin-degeneracy factors (i.e., isospin-hypercharge saturated matter). In all cases the hyperons get into the game at quite low densities, around $(2–3)\rho_0$ in accordance with previous works [1]. The composition is quite similar for all parameter sets studied up to $4\rho_0$. The effects coming from the inclusion of a scalar isovector meson $a_0(980)$ (in our notations δ) have been discussed. The equation of state does not change significantly but all the baryons have now different (nondegenerate) effective masses. The protons and electrons are getting slightly suppressed at lower densities and the electrochemical potential decreases while the Σ^-'s occur at somewhat lower densities compared to the model without the δ-meson contribution.

The possibility of antikaon condensation has been also studied within the framework of the relativistic mean-field model with a meson exchange interaction scheme. Fixing the vector coupling constants by SU(3) arguments, the in-medium energy of the antikaon was calculated for different choices of the K^- optical potential at normal nuclear density. The presence of hyperons, especially the repulsive contribution from ϕ exchange and the decrease of the electrochemical potential, make the antikaon condensed phase less favorable even at very high densities. For different parameter sets we get different answers concerning the presence of antikaons in the dense interior of neutron stars. Nevertheless, we find no onset of antikaon condensation below $\rho < 6\rho_0$ except for the set fitted to bulk nuclear matter (GL85) with an antikaon optical potential of $U_{\rm opt}^{\bar{K}} = -200$ MeV. Note that the maximum density of neutron star will set another limit for the kaon condensed phase which has not been studied here.

In a second approach we fix the coupling constants to the available KN-scattering data and take care of the off-shell behavior of the KN-scattering amplitude. Hence, this approach fulfills the low-density theorems for kaons. We have found that the effective energies of kaons and antikaons have a more or less standard behavior at low densities, but at $\rho = (3–4)\rho_0$ they bend due to the cancellation of the contributions from the different vector fields. For very high densities ($\rho > 7\rho_0$), when the contribution from the (hidden) strange meson field exceeds the one coming from the ω-meson field, it is even possible that the effective energy of the kaon becomes lower than that of the antikaon. Due to the nonlinear density dependence of the effective energy, the antikaon condensation does not occur in any of our parametrizations.

The extrapolation to hyperon-rich matter is associated

with large uncertainties due to the unknown hyperon-kaon interaction (e.g., $K\Xi$ interaction). The effective energy of the kaon is very much influenced by large cancellation effects coming from the vector fields. A slight increase of the coupling constants might therefore change the antikaon energy by 100 MeV which are at least missing for the onset of kaon condensation. Hence, there might still be some niches for antikaon condensation. Nevertheless, the overall trend is quite clear: the presence of hyperons makes the onset of antikaon condensation quite unlikely.

The vector self-interaction terms as well as the hyperon-hyperon interactions will influence also the maximum mass, the rotational frequency and cooling properties of neutron stars. These questions will be studied in a forthcoming work.

ACKNOWLEDGMENTS

We would like to thank Jakob Bondorf, Norman K. Glendenning, Dirk H. Rischke, Chris Pethick, Vesteinn Thorsson, Fridolin Weber, Wolfram Weise, and Thomas Waas for useful discussions and remarks. We thank Avraham Gal for a careful reading of the manuscript and clarifying remarks, especially about the K^- optical potential. This work was supported in part by the Carlsberg Foundation (Denmark), the International Science Foundation (Soros) Grant No. N8Z000 and EU-INTAS Grant No. 94-3405. J. Schaffner was supported by the EU program ''Human Capital and Mobility'' (Contract No. ERBCHBGCT930407). The authors also thank the Niels Bohr Institute for kind hospitality and financial support.

[1] N.K. Glendenning, Phys. Lett. **114B**, 392 (1982); Astrophys. J. **293**, 470 (1985); Z. Phys. A **326**, 57 (1987); F. Weber and N.K. Glendenning, *Proceedings of the International Summer School on Nuclear Astrophysics*, Tianjin, P.R. China (World Scientific, Singapore, 1991), pp. 64–183.
[2] A.R. Bodmer and C.E. Price, Nucl. Phys. **505**, 123 (1989).
[3] P.-G. Reinhard, Z. Phys. A **329**, 257 (1988).
[4] A.R. Bodmer, Nucl. Phys. **A526**, 703 (1991).
[5] Y. Sugahara and H. Toki, Nucl. Phys. **A579**, 557 (1994).
[6] S. Gmuca, J. Phys. G **17**, 1115 (1991); Z. Phys. A **342**, 387 (1991); Nucl. Phys. **A547**, 447 (1992).
[7] J. Schaffner, C.B. Dover, A. Gal, C. Greiner, and H. Stöcker, Phys. Rev. Lett. **71**, 1328 (1993).
[8] J. Schaffner, C.B. Dover, A. Gal, D.J. Millener, C. Greiner, and and H. Stöcker, Ann. Phys. (N.Y.) **235**, 35 (1994).
[9] D.B. Kaplan and A.E. Nelson, Phys. Lett. B **175**, 57 (1986); A.E. Nelson and D.B. Kaplan, *ibid.* **B192**, 193 (1987).
[10] G.E. Brown, K. Kubodera, M. Rho, and V. Thorsson, Phys. Lett. B **291**, 355 (1992); V. Thorsson, M. Prakash, and J.M. Lattimer, Nucl. Phys. **A572**, 693 (1994).
[11] G.E. Brown, C.-H. Lee, M. Rho, and V. Thorsson, Nucl. Phys. **A567**, 937 (1994).
[12] J. Schaffner, A. Gal, I.N. Mishustin, H. Stöcker, and W. Greiner, Phys. Lett. B **334**, 268 (1994).
[13] T. Muto, Prog. Theor. Phys. **89**, 415 (1993).
[14] P.J. Ellis, R. Knorren, and M. Prakash, Phys. Lett. B **349**, 11 (1995).
[15] B.D. Serot and J.D. Walecka, Adv. Nucl. Phys. **16**, 1 (1986); B.D. Serot, Rep. Prog. Phys. **55**, 1855 (1992).
[16] P.-G. Reinhard, Rep. Prog. Phys. **52**, 439 (1989).
[17] J. Boguta and A.R. Bodmer, Nucl. Phys. **A292**, 413 (1977); J. Boguta and H. Stöcker, Phys. Lett. **120B**, 289 (1983).
[18] M. Rufa, P.-G. Reinhard, J. Maruhn, W. Greiner, and M.R. Strayer, Phys. Rev. C **38**, 390 (1988).
[19] M.M. Sharma, M.A. Nagarajan, and P. Ring, Phys. Lett. B **312**, 377 (1993).
[20] R. Brockmann and W. Weise, Phys. Lett. **69B**, 167 (1977); J. Boguta and S. Bohrmann, *ibid.* **102B**, 93 (1981); M. Rufa, H. Stöcker, P.-G. Reinhard, J. Maruhn, and W. Greiner, J. Phys. G **13**, L143 (1987); J. Mareš and J. Žofka, Z. Phys. A **333**, 209 (1989); M. Rufa, J. Schaffner, J. Maruhn, H. Stöcker, W. Greiner, and P.-G. Reinhard, Phys. Rev. C **42**, 2469 (1990).
[21] N.K. Glendenning and S.A. Moszkowski, Phys. Rev. Lett. **67**, 2414 (1991).
[22] J. Schaffner, C. Greiner, and H. Stöcker, Phys. Rev. C **46**, 322 (1992).
[23] C.B. Dover, D.J. Millener, and A. Gal, Phys. Rep. **184**, 1 (1989).
[24] J. Mares, E. Friedman, A. Gal, and B.K. Jennings, TRIUMF Report No. TRI PP 95-15, nucl-th/9505003, 1995.
[25] A.R. Bodmer and Q.N. Usmani, Nucl. Phys. **A468**, 653 (1987).
[26] J.M. Lattimer, C.J. Pethick, M. Prakash, and P. Haensel, Phys. Rev. Lett. **66**, 2701 (1991).
[27] R. Machleidt, K. Holinde, and C. Elster, Phys. Rep. **149**, 1 (1987).
[28] R. Büttgen, K. Holinde, A. Müller-Groeling, J. Speth, and P. Wyborny, Nucl. Phys. **A506**, 586 (1990); A. Müller-Groeling, K. Holinde, and J. Speth, *ibid.* **A513**, 557 (1990).
[29] M. Lutz, A. Steiner, and W. Weise, Phys. Lett. B **278**, 29 (1992); Nucl. Phys. **A547**, 755 (1994).
[30] C.-H. Lee, H. Jung, D.-P. Min, and M. Rho, Phys. Lett. B **326**, 14 (1994), and references therein.
[31] C.-H. Lee, G.E. Brown, D.-P. Min, and M. Rho, Nucl. Phys. **A585**, 401 (1995).
[32] T. Maruyama, H. Fujii, T. Muto, and T. Tatsumi, Phys. Lett. B **337**, 19 (1994).
[33] E. Friedman, A. Gal, and C.J. Batty, Phys. Lett. B **308**, 6 (1993); Nucl. Phys. **A579**, 518 (1994)
[34] P.B. Siegel and W. Weise, Phys. Rev. C **38**, 2221 (1988).
[35] V. Koch, Phys. Lett. B **337**, 7 (1994).
[36] N. Kaiser, P.B. Siegel, and W. Weise, Technische Universität München Report No. TUM/T39-95-5, 1995.
[37] D.H. Rischke, Int. J. Mod. Phys. E **3**, 1157 (1994).
[38] T.A. Armstrong *et al.* WA76 Collaboration, Z. Phys. A **51**, 351 (1991).
[39] J. Cohen, Phys. Rev. C **39**, 2285 (1989).
[40] T. Barnes and E.S. Swanson, Phys. Rev. C **49**, 1166 (1994).
[41] J. Delorme, M. Ericson, and T.E.O. Ericson, Phys. Lett. B **291**, 379 (1992); H. Yabu, S. Nakamura, and K. Kubodera, *ibid.* **317**, 269 (1993); H. Yabu, S. Nakamura, F. Myhrer, and K. Kubodera, *ibid.* **B315**, 17 (1993).
[42] V. Thorsson and A. Wirzba, Nucl. Phys. **A589**, 633 (1995).